PROCEEDINGS B

royalsocietypublishing.org/journal/rspb

Research

Cite this article: O'Hara TD, Thuy B, Hugall AF. 2021 Relict from the Jurassic: new family of brittle-stars from a New Caledonian seamount. *Proc. R. Soc. B* **288**: 20210684. https://doi.org/10.1098/rspb.2021.0684

Received: 6 April 2021
Accepted: 21 May 2021

Subject Category:
Evolution

Subject Areas:
taxonomy and systematics, evolution

Keywords:
Ophiuroidea, palaeoendemism, deep-sea, phylogenomics, microfossil

Author for correspondence:
Timothy D. O'Hara
e-mail: tohara@museum.vic.gov.au

Electronic supplementary material is available online at https://doi.org/10.6084/m9.figshare.c.5448691.

THE ROYAL SOCIETY PUBLISHING

Relict from the Jurassic: new family of brittle-stars from a New Caledonian seamount

Timothy D. O'Hara[1], Ben Thuy[2] and Andrew F. Hugall[1]

[1]Department of Sciences, Museums Victoria, GPO Box 666, Melbourne, Victoria 3001, Australia
[2]Department of Palaeontology, Natural History Museum of Luxembourg, 24 Rue Münster, 2160 Luxembourg, Luxembourg

TDO, 0000-0003-0885-6578

The deep-seafloor in the tropical Indo-Pacific harbours a rich and diverse benthic fauna with numerous palaeoendemics. Here, we describe a new species, genus and family of brittle-star (Ophiuroidea) from a single eight-armed specimen collected from a depth between 360 and 560 m on Banc Durand, a seamount east of New Caledonia. Leveraging a robust, fossil-calibrated (265 kbp DNA) phylogeny for the Ophiuroidea, we estimate the new lineage diverged from other ophiacanthid families in the Late Triassic or Jurassic (median = 187–178 Myr, 95% CI = 215–143 Myr), a period of elevated diversification for this group. We further report very similar microfossil remains from Early Jurassic (180 Myr) sediments of Normandy, France. The discovery of a new ancient lineage in the relatively well-known Ophiuroidea indicates the importance of ongoing taxonomic research in the deep-sea, an environment increasingly threatened by human activities.

1. Introduction

The offshore banks and seamounts around New Caledonia are recognized for their rich diverse marine fauna, occurring both at sublittoral (0–200 m) and upper bathyal depths (200–1000 m) [1]. This fauna includes several phylogenetic relicts, which appear to be survivors of ancient faunal groups that have otherwise gone extinct. Examples include: one of the few surviving species of nautiloid cephalopods (now the marine emblem of New Caledonia); three of the eight extant species of cyrtocrinids, an order of crinoids that was highly diverse during the Mesozoic [2]; and one of the two modern species of glypheoid lobsters that otherwise went extinct in the Eocene [3]. This fauna has been discovered though the exceptional tropical deep-sea benthos (TDSB) programme led by the Muséum national d'Histoire naturelle (MNHN) and Institut de Recherche pour le Développement (IRD) who have conducted over 40 scientific surveys of the deep-sea environment around New Caledonia (http://expeditions.mnhn.fr/program/tropicaldeep-seabenthos).

Here, we describe a new species, genus and family of Ophiuroidea (brittle-stars) collected by the EXBODI expedition from the Durand Bank on the Loyalty Ridge, located in the south-west of the New Caledonian Exclusive Economic Zone. A recent phylogeny of living Ophiuroidea based on 265+ kbp of DNA sequence [4,5] allows us to place this new lineage within the tree of life with precision. The discovery that the external micro-structure of lateral arm plates (LAPs) is phylogenetically conserved on ophiuroids [6–9] facilitates a comparison with fossil taxa.

2. Material and methods

The holotype (and only known specimen) of the new species was collected on 13 September 2011 by 4 m beam trawl from the RV *Alis* on the EXBODI expedition (stn CP3849) on Banc Durand, New Caledonia (22°2.7′ S, 168°40.8′ E, 360–560 m). This bank is on the southern Loyalty Ridge and is likely of volcanic origin [10].

The bank is now partially covered in sediment on the flanks and coral reef on the flat summit, which lies just below the sea surface at approximately 10 m depth [11]. The specimen was fixed and preserved in ethanol and is stored at the MNHN, Paris, registration no. MNHN IE.2007.6821.

The microfossils were hand-picked from washing residues of sediments from the Lower Jurassic (Toarcian, Serpentinum and Bifrons Ammonite zones, 180 Myr) of Feuguerolles, Normandy, France (see [12] for site details). The fossil specimens are stored at the Natural History Museum of Le Mans (France) (collection acronym MHNLM).

We sequenced genomic DNA from the new specimen using the exon-capture procedure, as described in Hugall *et al.* [13] and http://dx.doi.org/10.5061/dryad.db339, with a minimum coverage limit of five reads. Following the approach taken in our previous phylogenomic analyses [4,5,14], we included this new data in a selection of 195 species representing all major lineages and family crown clades (electronic supplementary material, table S1). After standard data filtering [13] the final dataset comprised 265 158 sites in 1496 exons from 416 genes, with the 195 taxa and is 94% (median) complete. For computationally intensive Bayesian dating analyses we used a subset of 79 taxa (phylogenetically spread but focused on the Ophiacanthida) with a subset of 219 exons, one per gene, amounting to 45 981 sites (see electronic supplementary material, table S2 and references [5] and [15] for further details).

We generated phylogenetic trees using maximum-likelihood (RAxML v. 8.1.20) [16], Bayesian (BEAST v. 2.4.7) [17] and species tree approaches (ASTRAL II v. 5.5.10) [18], the latter used to assess artefacts of sequence concatenation [18]. All concatenated data RAxML and BEAST analyses used a three-part codon position GTR + G + F site rate heterogeneity model with base frequency estimation, as selected via ModelFinder in IQ-TREE [19]. Phylogenetic trees for both 195 taxa and 79 taxa are generated in RAxML by running 200 non-parametric bootstraps (the –f i command) that retain branch lengths per bootstrap. These analyses were run on the CIPRES supercomputing facility. As with our previous phylogenomic analyses, RAxML trees were *post hoc* rooted by splitting the branch between the two superorders Euryophiurida and Ophintegrida in proportion to the split estimated by the 425-gene echinoderm transcriptome phylogenomic study of O'Hara *et al.* [6]. These trees were then used in dating analyses described below.

Following O'Hara *et al.* [4] we also inferred a species tree using ASTRAL II, with local posterior support values [20], from 353 (the most data rich, electronic supplementary material, table S2) separate gene trees, drawn from the full 265 kb 195 taxa dataset. We used genes (rather than exons) as independent loci [21]. Unrooted gene trees were generated by RAxML (–f d command) using a single partition GTR + G + F model (due to reduced information per gene as compared to the full concatenated data). These gene datasets comprised (median) 189 taxa and 513 sites, with each of the 195 taxa having (median) 343 gene trees (330 for specimen IE.2007.6821). The ASTRAL species tree figure is presented as rooted for ease of comparison.

To investigate the accuracy and precision of dating the new lineage, we used both penalized likelihood rate smoothing (PLRS) [22] and Bayesian relaxed-clock methods (BEAST). Both the PLRS and BEAST analyses used slightly modified versions of previously published [4,5] calibrations (electronic supplementary material, table S3): 11 fossil-based node minimum constraints spread across most major lineages (invoked as either uniform, γ or exponential priors), plus a root secondary calibration normal prior (mean = 260.0, $\sigma = 7.0$ Ma) based on the results of O'Hara *et al.* [6].

PLRS is a widely used maximum-likelihood method for producing time-calibrated chronograms from phylogenetic trees but is not well-suited to providing uncertainty limits compared to Bayesian methods [23,24]. In order to provide some measure of uncertainty, we included three sources of variation: (1) 200 non-parametric bootstrap trees to account for branch length and topology uncertainty, (2) calibrated (in addition to minimum constraints) with a root age drawn from a normal prior distribution (above, as also used in BEAST analyses) and (3) smoothing factor drawn from a γ prior distribution ($\alpha = 1.5$, $\beta = 4.0$; median = 5.8), based on smoothing factor cross-validation distribution fit (reflecting uncertainty in the relaxed-clock model, [22]). PLRS was run in r8s v. 1.7 using the ADD penalty function and TN optimization. This approach was taken for both the 195 and 79 taxa trees, and trees and age distributions compared, focusing on the stem age distribution of the target sample (IE.2007.6821). These sets of 200 PLRS chronograms were then summarized as a maximum clade credibility (MCC) tree using FigTree v. 1.3.1 (http://tree.bio.ed.ac.uk/software/figtree).

Bayesian dating estimates were obtained using BEAST2 v.2.4.7 using sequence evolution data, relaxed-clock and calibration prior models similar to those used before [4,5,14]: a codon position GTR + G + F sequence evolution model, with log-normal relaxed-clock model and Yule tree prior (both using 1/X parameterization). Analyses used a PLRS tree as a starting tree and were *a priori* rooted by enforcing the reciprocal monophyly of the two superorders. Two independent runs of 100 M generations (1/10 000 sampling) were executed with 20% burnin, and assessed for convergence; each run returning posterior likelihood ESS greater than 100 [25]. The two runs used the alternate standard 'uniform' or 'exponential' versions of the fossil-based calibration constraints (electronic supplementary material, table S3). MCC trees and age distributions were evaluated separately and combined, focusing on the stem age distribution of the new species, and compared to the PLRS results. The full PLRS and BEAST MCC trees were presented in electronic supplementary material, figures S1 and S2.

Light images of the holotype were taken at Museums Victoria with a Visionary Digital Integrated System, using a Canon 5D Mark II camera with EF100 mm and MP-E65 mm macro-lenses, and montaged using Zerene Stacker v. 1.04 software. Ossicles of the arm skeleton were extracted from a proximal arm portion of the holotype, macerated in household bleach and rinsed in tap water, then mounted on aluminium stubs and gold-coated [8]. Scanning electron microscope (SEM) images were taken with a JEOL Neoscope JCM-5000 at the Natural History Museum Luxembourg.

Micro-CT scanning was performed with a Phoenix Nanotom m operated using xs control and Phoenix datos|x acquisition software (Waygate Technologies). The specimen was mounted by wrapping in ethanol soak gauze, secured by bubble wrap, and placed within a plastic specimen jar. An X-ray energy of 50 kV and 300 mA was used for two separate scans, one at a coarser voxel resolution of 25 µm to capture the full body of the specimen, and a higher resolution scan at 10 µm focusing on a region of interest encompassing the main body. Scans were run for 10 min in a fast scan mode collecting 1200 projections through a 360° rotation of the specimen. Volume reconstruction of the micro-CT data was performed using Phoenix datos|x reconstruction software (Waygate Technologies) applying an inline median filter and ROI filter during reconstruction. The data were exported as 16-bit volume files for imaging and analysis in Avizo (Thermo Fisher Scientific).

3. Nomenclatural acts

This published work and the nomenclatural acts it contains have been registered in ZooBank, the proposed online registration system for the International Code of Zoological

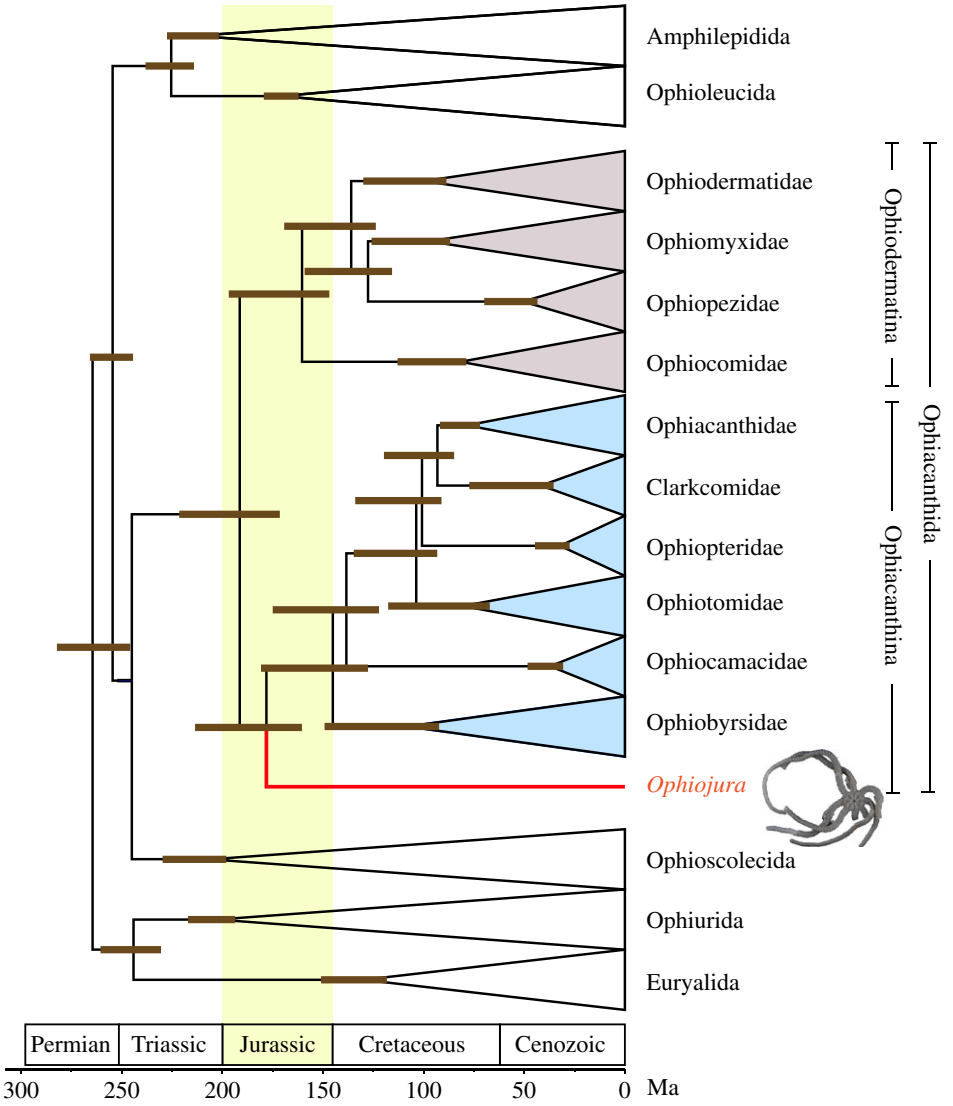

Figure 1. Phylogeny of the Ophiuroidea showing the position and estimated node age range (bars on nodes) of *Ophiojura* for the RAxML/PLRS 195-taxon analysis. Width of the collapsed clades not scaled to richness. All nodes are fully supported on the 195- and 79-taxon RAxML (bootstrap), BEAST (posterior) and ASTRAL II (local posterior), except the *Ophiojura* node which has values of 70, 79, 1.00 and 1.00, respectively. (Online version in colour.)

Nomenclature (ICZN). The ZooBank LSID (Life Science Identifiers) for this publication is (urn:lsid:zoobank.org:pub:7DC3B82F-C07A-483B-A1C5-8FDEEB718938). LSIDs for the new taxa are given below.

4. Results

(a) Phylogenetic analyses

From the only known specimen we obtained 89% of our exon-capture target of 265 158 bp. RAxML bootstrap support for the position of the new species as sister to the rest of the suborder Ophiacanthina was 70%/79% in the 195/79 taxa analyses (figure 1; electronic supplementary material, figure S1*a*,S2*a*). Both the ASTRAL species tree (electronic supplementary material, figure S1*b*) and BEAST relaxed-clock tree (electronic supplementary material, figure S2*b*) returned this position, with posterior supports of 1.00. The remainder (minority) of the RAxML bootstraps placed the new species as sister to Ophiodermatina (rather than Ophiacanthina), hence complete support for it lying within the Ophiacanthida order crown as defined by O'Hara *et al.* [4,14]. As support for nodes above and below this rank is in all cases unanimous, we can exclude the new species from lying within or on the stem of any single described family (in particular the Ophiobyrsidae).

Our previous fast bootstrap GTRCAT model analysis [5] returned approximately 90% support for the position of the new species, broadly in proportion to the non-parametric bootstrap as is theoretically expected of such methodology (70–95% [16,26]). The difference between thorough bootstrap analyses likely reflects taxon sampling [27]. The significant species tree local posterior support (1.00) compared to the slightly equivocal bootstrap may be expected of a short internode due to a short time interval relative to the mutation/fixation process [21]. Hence the new species can confidently be placed as the sister to all currently known Ophiacanthina and therefore must belong to a distinct family.

Results of the dating are summarized in figure 2. The dating of the new species node was very similar between different methods, taxon sets and priors, *viz* PLRS ($n = 195$ taxa): median = 180 (95% CI = 163–215), PLRS(79): 178 (154–205), BEAST-Uniform(79): 187 (149–211), BEAST-Exponential(79): 181 (143–215) Myr. This consistency suggests that methodological issues are not critical but the results have limited precision. While we have considerable data to estimate topology and branch length, our calibrations are broad, and perhaps more importantly, there is considerable apparent rate variation

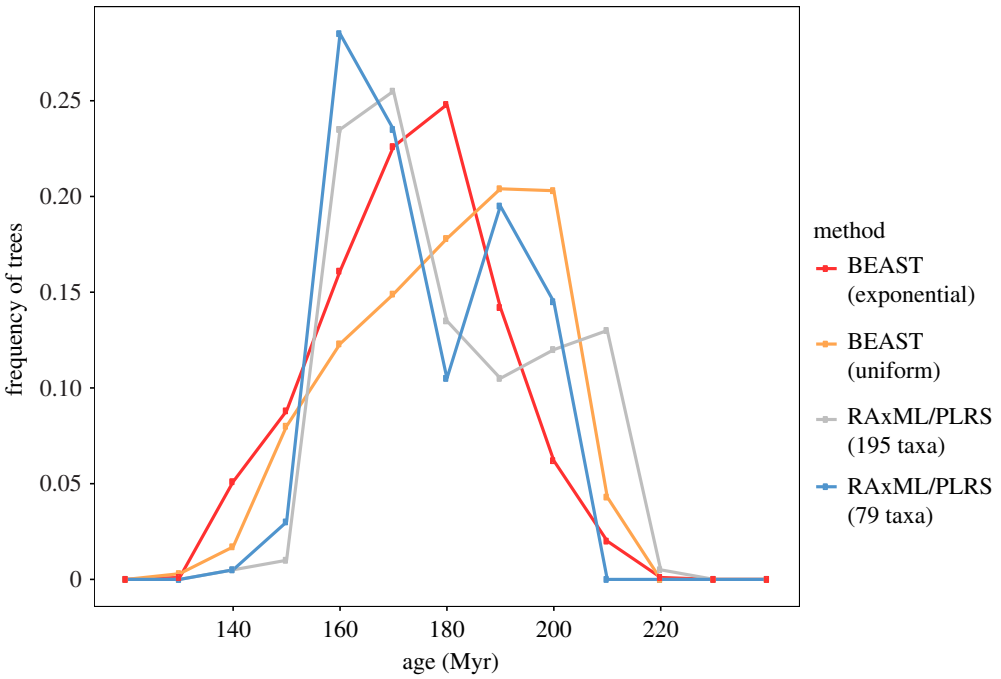

Figure 2. *Ophiojura* lineage age dating estimate distributions. PLRS transformed RAxML trees from the full 265 kb exon data with either 195 or 79 taxa, BEAST analyses used 79 taxa with the reduced 46 kb exon data, using either the standard 'uniform' prior or 'exponential' prior age calibration sets. Drawn from 200 PLRS trees and 1000 BEAST posterior tree samples in 10 Myr bins. (Online version in colour.)

among major lineages—(see non-clock trees in [4–6,13]). Such variation inevitably creates complex solutions for any relaxed-clock model, even when there are precise calibrations [23,24]. Some of this can be seen in the age distributions (figure 2) with a bimodal pattern in PLRS and broad distributions and relatively poor ESS per MCMC chain length in the BEAST results. Nevertheless, in all cases the 95% CI fall mainly within the Jurassic Period and it is the oldest single species (longest branch, electronic supplementary material, figure S3) in our global sample of nearly 1000 ophiuroid species [5].

5. Systematic taxonomy

Phylum: Echinodermata
Class: Ophiuroidea
Order: Ophiacanthida
Suborder: Ophiacanthina
Family: Ophiojuridae fam. nov.
urn:lsid:zoobank.org:act: 5854ACA1-6994-4379-88DF-FA2F3F53E891
Genus: *Ophiojura* gen.nov.
urn:lsid:zoobank.org:act: EE0F43F8-0773-4641-A47A-D9BDF0AD4386
Species: *Ophiojura exbodi* sp. nov.
urn:lsid:zoobank.org:act: D83078F6-A23D-41EF-B2BA-3094159B2F5A.

(a) Holotype and type locality data

Registration no.: MNHN IE.2007.6821. EXBODI stn CP3849, Banc Durand, New Caledonia, 22°2.7′ S, 168°40.8′ E, 360–560 m, 13 September 2011.

(b) Etymology

The genus and family are named after the Jura Mountains (noun), type locality for the Jurassic period, with the prefix 'Ophio' derived from the Ancient Greek word for serpent. The species is named after the EXBODI expedition (noun) that collected the holotype, organized by Dr Sarah Samadi of MNHN, Paris.

(c) Family and genus diagnosis

LAPs higher than long, with a long proximal extension that curves around the large open tentacle pore (figure 3*f*,*h*). Arm spine articulations a distinctive 'pig-snout'-shape (figure 4*a*,*c*), with a large muscle opening bordered ventro-proximally by a small, thin ventral lobe, a much larger, swollen lobe dorsally bordering both the muscle opening and the slightly smaller and widely separated nerve opening. Distinctive hook-shaped arm spines on distal arm segments, with nerve and muscle attachments, two rows of thorns and a large, recurved terminal claw. Contiguous ventral arm plates (VAPs), longer than wide, constricted laterally around the tentacle pores (figure 3*f*). Dorsal arm epidermis contains perforated thin ossicles over the vertebrae but no solid plates (figure 3*e*). Vertebrae with zygospondylous (yoke-shaped) articulation (figure 4*h*,*i*). Oral and tooth papillae with a spine-like core surrounded in soft tissue (figure 3*d*). Three peristomial plates that sit dorsally over the water vascular ring/neural groove (figure 3*g*).

(d) Holotype description

Disc diameter estimated (from remnant pieces) to be at least 30 mm, longest arm piece greater than 80 mm (from mouth centre, 45 segments). Eight arms (figure 3*a*,*b*), 3.4 mm across at base. Colour pale tan/white, no indication of any pigmented markings. Dorsal disc mostly absent, small remaining pieces attached to arms are composed of thick dermis typically without spines or plates, although one piece has a tiny oval plate that may be the radial shield. No sign of any remaining genital plate.

Jaws elongate, 3.7 mm long, 3 mm wide at base. Adoral shields long and narrow, extending from half the length of

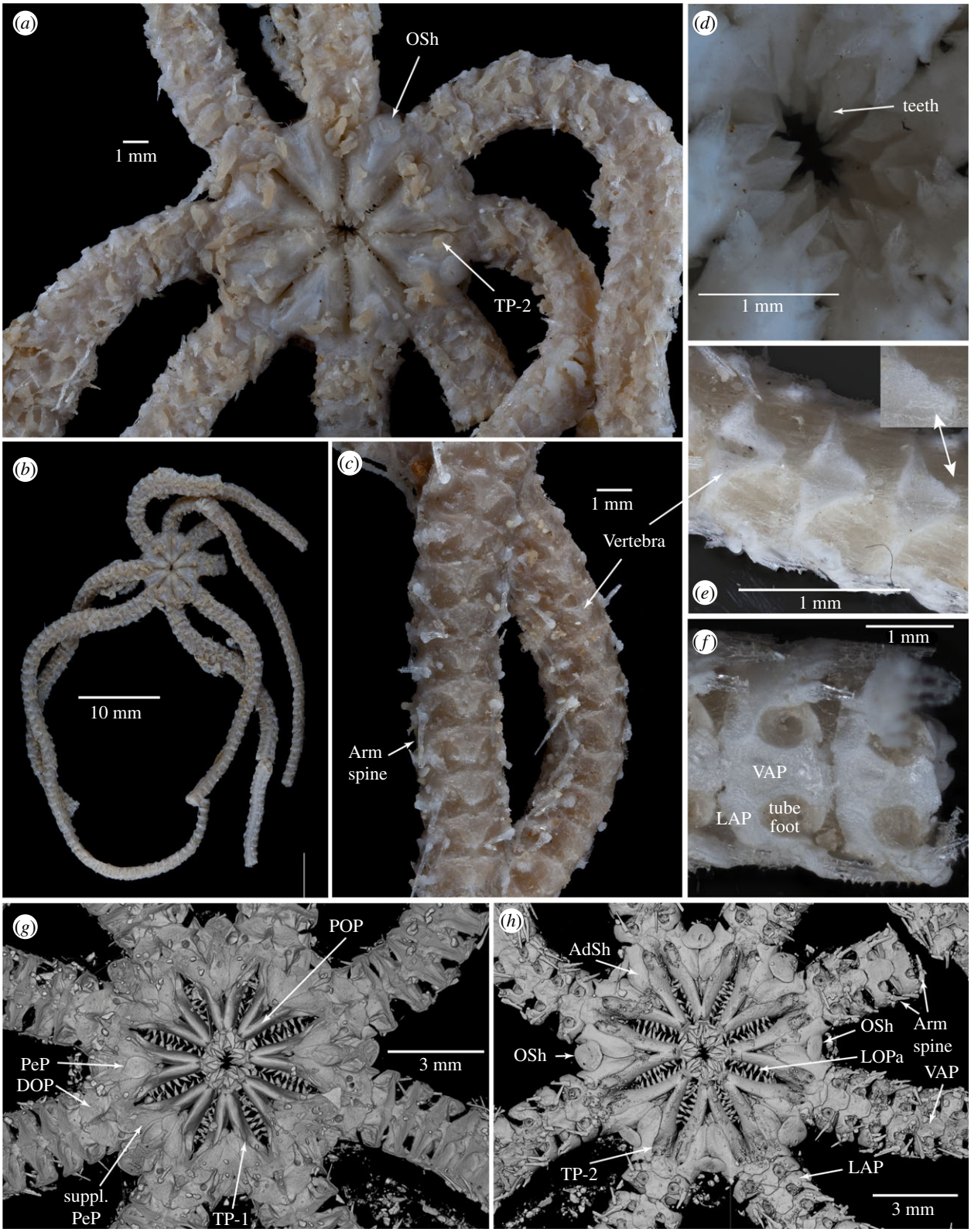

Figure 3. *Ophiojura exbodi* (MNHN IE.2007.6821) holotype. (*a*) Ventral view of disc, (*b*) ventral view of animal including remaining arm fragments, (*c*) dorsal view of arms, (*d*) teeth papillae, (*e*,*f*) partially macerated arm segments from mid arm, (*e*) in dorsal view, with inset showing small perforated epidermal plates, (*f*) ventral view. Rendered CT scan of the (*g*) dorsal and (*h*) ventral surfaces. AdSh, adoral shield; DOP, distal oral plate element; LAP, lateral arm plate; LOPa, lateral oral papillae, OSh, oral shield; PEP, peristomial plate; POP, proximal oral plate element; TP, tentacle pore; VAP, ventral arm plate. (Online version in colour.)

the jaw past the oral shield, meeting proximally, widely separated distally, with a truncate to concave distal margin (figure 3*h*). Ventral jaw surface proximal to adorals and between lateral oral plates is covered in skin. Oral shields 2× wider than long, convex proximally, truncate distally with rounded lateral angles, depressed in centre, four are larger (presumably madreporites), almost as long as wide, rounded, orientated obliquely to jaw (figure 3*h*). Cluster of four to six tooth papillae at jaw apex, each with an inner-spine-like core that is covered in a conical skin sheath, the inner-spine terminating in one or more thorns that emerge from the skin layer (figure 3*d*). A row of five teeth in vertical series widened at base but tapering to a point, followed by a cluster of three spine-like dorsal teeth (electronic

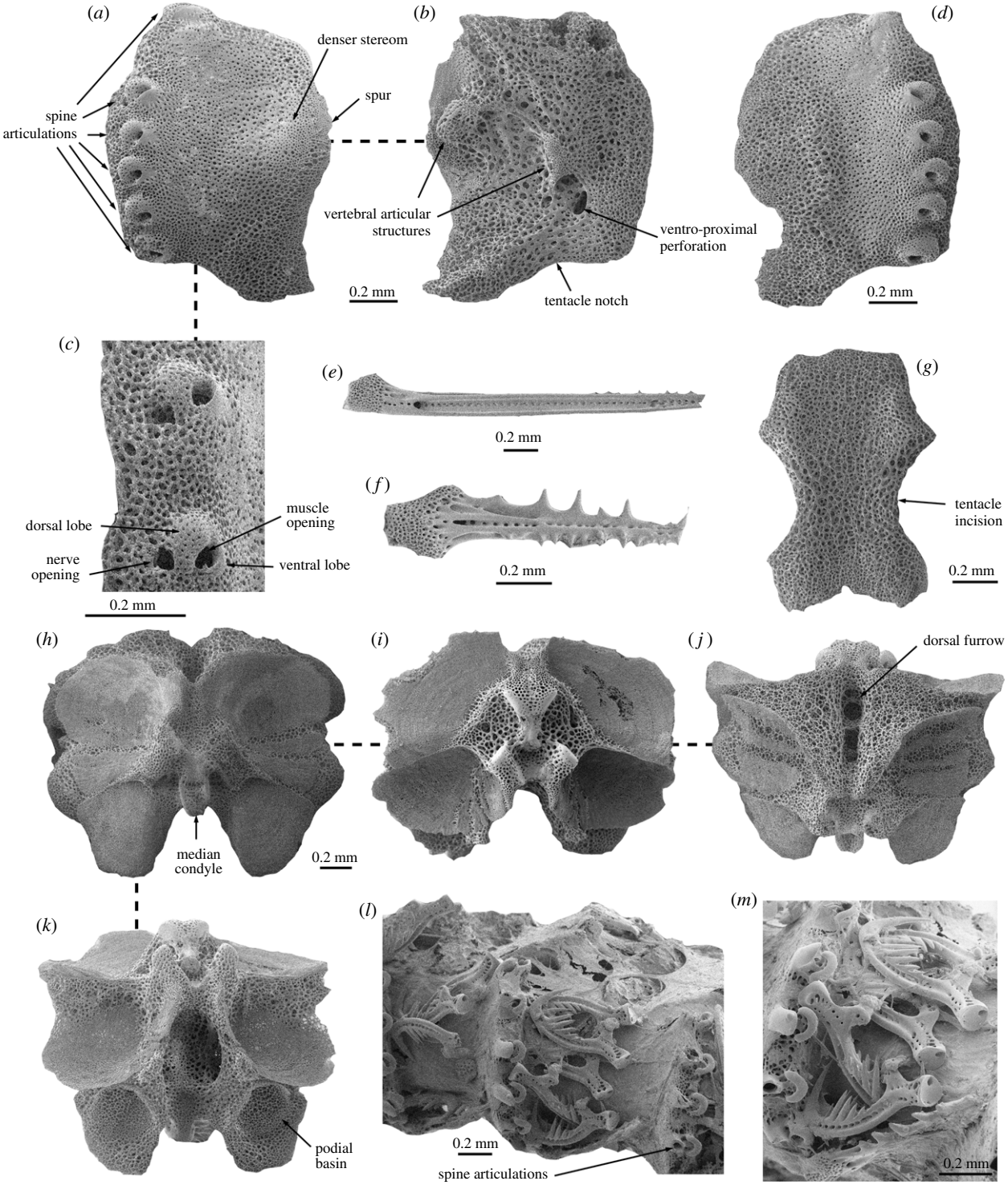

Figure 4. *Ophiojura exbodi* (MNHN IE.2007.6821) holotype. (*a–k*) SEMS of internal ossicles from the proximal to middle of the arm. (*a–d*) Lateral arm plates with dorsal side upwards and distal side with arm spine articulations, (*a*) external, (*b*) internal views of proximal plate, (*c*) detail of lower spine articulations, (*d*) external view from the middle of the arm. (*e*,*f*) Arm spines, (*e*) dorsal-most and (*f*) ventral spines. (*g*) Ventral arm plate in external view, with distal side upwards. (*h–k*) Vertebrae, (*h*) distal with dorsal side up, (*i*) proximal with dorsal side up, (*j*) dorsal with proximal side up and (*k*) ventral views (with proximal side up). (*l*,*m*) Distal arm segments with dorsal side up and distal side to the right, showing hook-shaped arm spines.

supplementary material, figure S5*a*,*b*). Exposed proximal end of the oral plates long and rounded on the ventral surface, forming elongated jaws and narrowly articulating radially before their proximal extent leaving a cavity between the oral and dental plates. The distal section of the oral plates have large dorsal extensions for inter-vertebral muscle attachments (higher than succeeding vertebrae) and a single dorsal foramen for the buccal water vascular canal on the abradial side that bifurcates within the oral plate to serve both the first (dorsal) and second (ventral) oral tentacles (electronic supplementary material, figures S4 and S5). The seven to eight oral papillae occur deep in the jaw slit along the lateral ridge of the oral plate, interleaving with series on opposing jaw. These papillae also have a spine-like core with a triangular skin sheath that is webbed to their neighbour at their bases. Distal third of jaw slit without oral papillae. One remaining spiniform adoral shield spine still present adjacent to 2nd oral tentacle pore, well outside of the jaw silt. The water vascular ring/neural groove protected dorsally by five overlapping plates (electronic supplementary material, figures S4 and S5), two falcate plates

[28] on the proximal side of the groove that also protect the dorsal side of the first tentacle, two supplementary peristomial plates that sit over the groove, and a central droplet-shaped peristomial plate that sits over the external interradial muscle [29] and possibly the stone canal.

No dorsal arm plates (DAPs, figure 3*c*), although some microscopic perforated ossicles appear to be embedded in the epidermis above and near the vertebrae (figure 3*e*). LAPs roughly ovoid, higher than long (0.8 × 0.68 mm) with a concave ventral border and a protruding ventro-proximal tip (figure 4*a*, *d*) that is contiguous with the VAP. A small rise dorso-proximally with denser stereom and a poorly defined, weakly prominent spur on the proximal edge of the LAP (figure 4*a*,*d*). Six arm spine articulations on flattened distal surface of LAP (figure 4*a*,*d*), each with a large muscle opening bordered ventro-proximally by a small, thin ventral lobe, a much larger, swollen dorsal lobe dorsally bordering both the muscle opening and the slightly smaller nerve opening, widely separating both openings to form a distinctive 'pig-snout'-shaped spine articulation (figure 4*c*). Distance between spine articulations strongly increasing dorsal-wards, with dorsal-most spine articulation widely separated from the other five. Interior LAP surface with two knob-shaped vertebral articular structures of dense stereom, one central and one near the distal margin and a ventro-proximal perforation (figure 4*b*). VAPs composed of open stereom, 2.0 mm long, 1.4 mm wide at widest point, 0.75 mm wide at narrowest point (figures 3*f* and 4*g*). Distally truncate, with distal-ward-divergent lateral sides, constricted mid-length around the large open tentacle pores, proximally flared, with a concave proximal border.

Six arm spines. Upper arm spine (2.1 mm) with base slightly enlarged of open stereom, shaft with a shallow wide furrow along the dorsal side with a proximal pore and series of stereom pores along its length, some small denticulations laterally near the tip (figure 4*e*). Five ventral spines, subequal (1.2 mm), with an expanded base, and central series of stereom holes along a narrow groove, denticulations prominent laterally, long along dorsal side, including from the truncate apex (figure 4*f*). On distal arm segments, four to five dorsal arm spines replaced by distinctive, hyaline hooks (figure 4*l*,*m*), composed of a coarsely porous base with a nerve opening and a lateral muscle attachment extension, followed by two rows of thorns apically converging into a large, recurved terminal thorn. Some hooks of the same LAP seemingly opposable. No tentacle scales observed.

Vertebrae with zygospondylous articulation, distal face with two lateral articulation surfaces and a median condyle with a concave face (figure 4*h*), proximal surface with median transverse bar and two ventral protuberances (figure 4*i*). Large dorsal and ventral muscle fossae, dorsal one with three to four areas of denser stereom. Deep dorsal furrow down the midline with several large apertures in the centre (figure 4*j*). Dorsal lateral wings relatively flat without pronounced curved grooves, nodulated external surface. Large podial basins (figure 4*k*).

(e) Extant relationships

The unusual 'pig-snout' form of the arm spine articulations is similar to *Ophiobyrsa rudis* Lyman, 1878, the type species of the type genus of Ophiobyrsidae [7]. The new species also shares other anatomical features with species within the Ophiobyrsidae as defined in O'Hara *et al*. [14], including the shape of the jaw, a series of pointed oral papillae along the oral plate ridge, a cluster of similar-shaped tooth papillae at the jaw apex, an adoral shield spine, reduced or absent DAPs, elongated contiguous VAPs, large tentacle pores that lack scales and reduced denticulate arm spines [7,30]. However, the vertebral articulation in the Ophiobyrsidae has been described as being streptospondylous (with hourglass-shaped articulation surfaces and no median condyle) [7,30]. The organization of the teeth can differ within that family, and there can be one to four vertical rows of teeth. Another important difference pertains to the ornamentation of the LAP external surface, the new species has areas of denser stereom and a spur on the proximal edge which are absent in the Ophiobyrsidae. The muscle and nerve openings of the spine articulations of the Ophiobyrsidae also tend to be separated by a thin, low ridge, whereas in the spine articulations of the new species, the muscle and nerve openings are separated by a much wider, swollen ventral-ward expansion of the dorsal lobe.

The Ophiocamacidae can have a cluster of tooth papillae, but in general *Ophiocamax* species have a more obvious ophiacanthid morphology, especially in having a single column of teeth dorsally, oral papillae on the ventrolateral edge of the oral plate, small tentacle pores, multiple tentacle scales, robust arm spines, robust DAPs, an armoured disc and volute-shaped arm spine articulations. The taxonomic distinction of large- and small-pored Ophiacanthids (*sensu* [31]) is not congruent with the latest molecular trees [4,14], as large pores can also occur in the extant Ophiotomidae (e.g. *Ophiotoma* and *Ophiopristis* species).

The other families within the Ophiacanthida have a disc either covered in plates or spines/granules, the tentacle pores on the arm are typically small and covered by tentacle scales (with a few exceptions, most notably *Ophiotoma*) and the teeth and oral papillae are generally solid, blunt or rounded. Furthermore, the Clarkcomidae and Ophiopteridae have their oral frame modified into a 'buccal funnel' [28] to crush food before ingestion, with ventral teeth modified into multiple rows of blunt papillae.

The new species also bears some resemblance to species in the Ophioscolecida (historically placed in a polyphyletic Ophiomyxidae), including the large tentacle pores, presence of tooth papillae, lack of flabelliform teeth, oral papillae that form along the oral plate ridge (rather than on a ventrolateral margin), the large 2nd oral pore with a podia that cannot enter the mouth slit when closed and the presence of an adoral shield spine [7,14,28]. The genus *Ophioleptoplax* in particular has a similar oral frame, VAPs, tentacle pores and reduced DAPs. However, it differs in having long smooth solid arm spines. It supposedly has no radial shields, but this was doubted by Martynov who discovered minute radial shields in similar species [7].

Multiple unbranched arms are unusual in the Ophiuroidea but their presence is not significant for higher-level classification. Of the almost 2100 accepted species of Ophiuroidea, only four species *Astrochlamys sol* Mortensen, 1936, *A. timoharai* Okaniski & Mah, 2020 (Order Euryalida), *Soliophis bakeri* Okanishi & Mah, 2020 (Ophioscolecida) and *Ophiacantha decaactis* Belyaev & Litvinova, 1976 (Ophiacanthida) have been recorded with 10 or more simple arms; one *Ophiacantha enneactis* H.L. Clark, 1911 with nine; and two species *Ophiacantha opulenta* Koehler, 1908; *Ophiacantha vivipara kerguelensis* Studer, 1876 can rarely have up to eight arms. Some fissiparous species, which usually have six arms, have also been recorded occasionally with

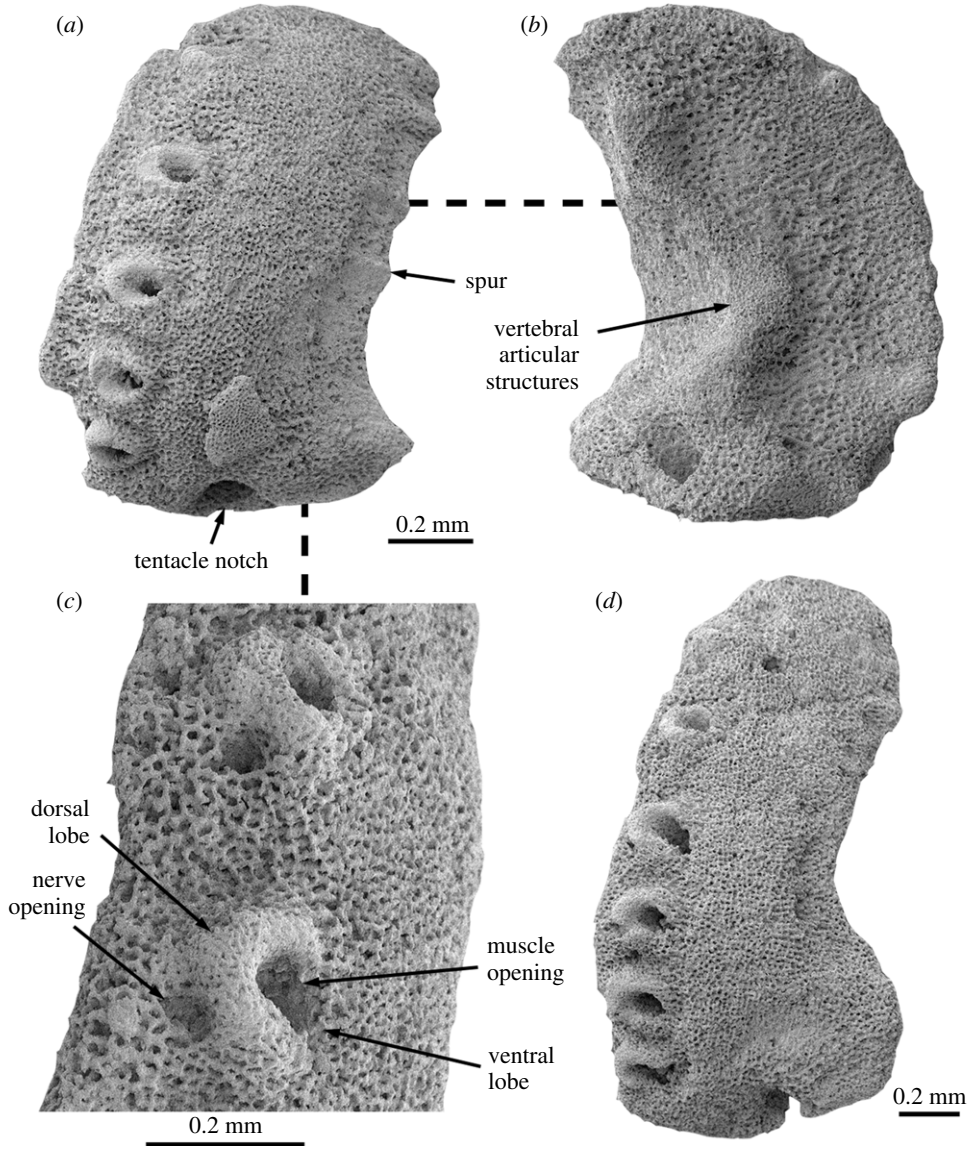

Figure 5. Fossil Ophiojuridae from the Lower Jurassic (Toarcian, Serpentinum and Bifrons ammonite zones, 180 Myr) of Feuguerolles, Normandy, France. SEMs of lateral arm plate microfossils with dorsal side up. (*a–c*) MHNLM 2020.1.4, proximal to median lateral arm plate in (*a*) external and (*b*) internal view and (*c*) with detail of spine articulations. (*d*) MHNLM 2020.1.5, proximal lateral arm plate in external view.

seven, including *Ophiocomella sexradia* (Duncan, 1887) (Ophiacanthida) and various *Ophiactis* species (Amphilepidida). The presence of 10 or more simple arms has been associated with an arborescent habitat [32].

Wilkie & Brogger [29] have divided ophiuroid oral frames into two broad categories. *Ophiojura* conforms to type 'A' with spine-like teeth, oral plates with distally projecting oral and aboral convexities, and large peristomial plates that cover the circum-oral water vascular ring. Since this is the likely ancestral state [29], it is not a good indicator of phylogenetic relationships. Of the few figured species, the triple peristomial plate arrangement is reminiscent of that in *Ophioderma rubicunda* ([28], fig. 12*h*) in the suborder Ophiodermatina, although in that case the jaw is much shorter and the central peristomial plate small and triangular.

(f) Fossil relationships

The LAPs of the new species are very similar to previously unpublished microfossils from Lower Jurassic (180 Myr) of Feuguerolles, France (figure 5). The distinctive morphology of these LAP microfossils, including the 'pig-snout' form of the spine articulations with a thick ventral-ward extension of the dorsal lobe separating the muscle and nerve openings, and the presence of differentiated stereom and spurs on the external LAP surface, are consistent with the new family Ophiojuridae. These microfossil LAPs appear to be more heavily calcified than their extant counterparts, with thicker plates and more developed vertebral articular surface and tentacle notch.

Previously published LAP microfossils with 'pig-snout'-shaped spine articulations, all assigned to the extinct genus *Ophiojagtus* [31], differ in lacking external surface ornamentation and in having the muscle and nerve openings separated by a thin, low ridge, suggesting assignment to the Ophiobyrsidae. Furthermore, at least in the case of *Ophiojagtus argoviensis* (Hess, 1966), the associated vertebrae have a streptospondylous articulation corroborating the ophiobyrsid affinities.

6. Discussion

We have established a new family of brittle-stars based on a single damaged specimen. While this is not typical taxonomic

practice, we justify publication on the basis of robust phylogenomic and detailed morphological data, and to facilitate the collection and identification of new specimens. The situation is similar to the first description of an extant glypheoid lobster, based on one old dry specimen found in the Smithsonian Museum [33], which subsequently inspired a French expedition to the Philippines to locate more material [34].

Our phylogenetic analyses estimate that the *Ophiojura* lineage arose in the Jurassic or late Triassic periods, most probably from 160 to 200 Myr. It is the longest branch for any single species on our extensive molecular phylogeny of the Ophiuroidea [5]. Despite the substantial survey effort that has occurred in New Caledonian waters, we are unaware of any other specimen that could plausibly be confamilial with this specimen.

The fossil record indicates that the Jurassic was a period of elevated diversification of early ophiacanthid lineages, with many species occurring in the relatively shallow water of the continental shelves (0–200 m) [31]. The Ophiojuridae fossils presented herein confirm that the family was present by the Early Jurassic (180 Myr). However, several other derived ophiacanthid clades have a confirmed Early Jurassic fossil record [31], implying that the Ophiojuridae must have diverged before this period. Fossil and molecular evidence [35] has shown that the majority of the extant ophiacanthid clades originated in deeper waters (below 200 m), implying that their occurrence at shallower depths in the Jurassic represented a temporary expansion of their bathymetric range [31]. The fossil record is yet too sparse to confirm a similar pattern for the Ophiojuridae.

It is noteworthy, however, that the only known fossils of the Ophiojuridae were found in strata that yielded one of the oldest diversified shallow-water cyrtocrinid faunas [36]. Cyrtocinids, in fact, are another clade with an assumed deep-water origin followed by a temporary expansion to the shallow epicontinental seas of the Jurassic [36]. We, therefore, speculate that additional fossil members of the Ophiojuridae which bridge the extensive temporal gap between the Jurassic and the present, may be found either in the extremely poorly sampled deep-sea fossil record, or in ancient shelf settings affected by increased bathymetric faunal exchange [31].

Although the *Ophiojura* lineage is ancient, and the taxa is not known to have any close extant relatives, this does not imply that *Ophiojura* is 'primitive' [37] or that all its characters were present in the middle Jurassic. In particular, the presence of eight arms is not an indicator of deep taxonomic relationships. On the other hand, arm spine articulation morphologies do reflect the higher classification of the Ophiuroidea [6] and the shape outlined here may be an indicator of which of the many Jurassic fossils actually belong to the stem of the extant Ophiacanthina.

The discovery of a new lineage on a seamount could be seen as evidence for the hypothesis that seamount faunas can be highly endemic [1], reflecting the age and geographical isolation of the seamounts. However, initial reports that endemism is a feature of seamounts have not been supported by more detailed studies [38]. Many seamount species are widespread and apparently good dispersers [38]. Nor do seamounts have consistently higher species richness than areas of continental slope [39].

However, our new discovery does reflect the deep and rich evolutionary diversity that is present in the upper tropical bathyal of the Indo-Pacific [40]. This biome, particularly between 200 and 1000 m, is a reservoir of palaeoendemism (formerly widespread but now restricted lineages) both for ophiuroids [40] and other taxa (see introduction). Banc Durand, the type location of *Ophiojura*, also has been noted as a hotspot of octocoral phylodiversity [41]. To protect the rich tropical deep-sea fauna, the entire New Caledonia Exclusive Economic Zone was placed in 2014 within a vast marine protected area, the Coral Sea Nature Park.

Data accessibility. Input and output files from the phylogenetic analyses and images from the micro-CT scan of the holotype, the latter including stacked vertical and horizontal images, rendered images of the dorsal and ventral surfaces, and a rotating animation, are available from the Dryad Digital Repository: https://doi.org/10.5061/dryad.18931zcx3 [15]. Lists of materials, fossil calibration points and expanded phylogenetic trees are provided as electronic supplementary material. Requests to examine specimens can be directed to the relevant museum collection (MNHN and MHNLM).

The data are provided in the electronic supplementary material [42].

Authors' contributions. T.D.O.: conceptualization, data curation, formal analysis, investigation, methodology, project administration, resources, supervision, visualization, writing-original draft, writing-review and editing; B.T.: formal analysis, investigation, methodology, resources, writing-original draft, writing-review and editing; A.F.H.: formal analysis, investigation, methodology, writing-original draft, writing-review and editing.

All authors gave final approval for publication and agreed to be held accountable for the work performed therein.

Competing interests. The authors declare no competing interests.

Funding. Muséum national d'Histoire naturelle, Paris provided funding to identify specimens from expeditions to New Caledonia. The Australian National Environmental Science Program's (NESP) Marine Biodiversity Hub provided funding to sequence the taxonomic diversity of the Ophiuroidea around Australia and neighbouring nations.

Acknowledgements. We thank the scientists and collection managers of the Muséum national d'Histoire naturelle, Paris who have collected, preserved and curated the extraordinary deep-sea fauna around New Caledonia; the Melbourne TrACEES (Trace Analysis for Chemical, Earth and Environmental Sciences) Platform for access to the micro-CT scanner and Dr Jay Black (University of Melbourne) for technical support; Caroline Harding and Mark Nikolic (Museums Victoria) with assistance with the macro photography, and Marc Chesnier (Cresserons, France) who collected the fossil material.

References

1. Richer de Forges B, Koslow JA, Poore GCB. 2000 Diversity and endemism of the benthic seamount fauna in the southwest Pacific. *Nature* **405**, 944–947. (doi:10.1038/35016066)
2. Messing CG, Hoggett AK, Vail LL, Rouse GW, Rowe FWE. 2017 Class Crinoidea. In *Australian echinoderms: biology, ecology and evolution* (eds M Byrne, TD O'Hara), pp. 171–228. Melbourne, Australia: CSIRO Publishing and ABRS.
3. Boisselier-Dubayle MC, Bonillo C, Cruaud C, Couloux A, de Forges BR, Vidal N. 2010 The phylogenetic position of the 'living fossils' *Neoglyphea* and *Laurentaeglyphea* (Decapoda: Glypheidea). *C. R. Biol.* **333**, 755–759. (doi:10.1016/j.crvi.2010.08.007)
4. O'Hara TD, Hugall AF, Thuy B, Stöhr S, Martynov AV. 2017 Restructuring higher taxonomy using broad-scale phylogenomics: the living Ophiuroidea. *Mol.*

Phylogenet. Evol. **107**, 415–430. (doi:10.1016/j.ympev.2016.12.006)

5. Christodoulou M, O'Hara TD, Hugall AF, Arbizu PM. 2019 Dark ophiuroid biodiversity in a prospective abyssal mine field. *Curr. Biol.* **29**, 3909–3912.e3. (doi:10.1016/j.cub.2019.09.012)
6. O'Hara TD, Hugall AF, Thuy B, Moussalli A. 2014 Phylogenomic resolution of the class Ophiuroidea unlocks a global microfossil record. *Curr. Biol.* **24**, 1874–1879. (doi:10.1016/j.cub.2014.06.060)
7. Martynov AV. 2010 Reassessment of the classification of the Ophiuroidea (Echinodermata), based on morphological characters. I. General character evaluation and delineation of the families Ophiomyxidae and Ophiacanthidae. *Zootaxa* **2697**, 1–154. (doi:10.11646/zootaxa.2697.1.1)
8. Thuy B, Stöhr S. 2011 Lateral arm plate morphology in brittle stars (Echinodermata: Ophiuroidea): new perspectives for ophiuroid micropalaeontology and classification. *Zootaxa* **3013**, 1–47. (doi:10.11646/zootaxa.3013.1.1)
9. Thuy B, Stöhr S. 2016 A new morphological phylogeny of the Ophiuroidea (Echinodermata) accords with molecular evidence and renders microfossils accessible for cladistics. *PLoS ONE* **11**, e0156140. (doi:10.1371/journal.pone.0156140)
10. Bitoun G, Recy J. 1982 *Origine et évolution du bassin des Loyauté et de ses bordures après la mise en place de la série ophiolitique de Nouvelle Calédonie*. In *Contribution à Mude géodynamique du sud-ouest Pacifique Travaux et Documents de l'ORSTOM 147*, *Paris*, pp. 505–554.
11. Andréfouët S, Cabioch G, Flamand B, Pelletier B. 2009 The diversity of New Caledonia coral reef geomorphology and genetic processes: a synthesis from optical remote sensing, coring and acoustic multi-beam observations. *Coral Reefs* **28**, 691–707. (doi:10.1007/s00338-009-0503-y)
12. Hess H, Thuy B. 2017 Extraordinary diversity of feather stars (Echinodermata: Crinoidea: Comatulida) from a Lower Jurassic (Pliensbachian–Toarcian) rock reef of Feuguerolles (Normandy, France). *Swiss J. Palaeontol.* **136**, 301–321. (doi:10.1007/s13358-016-0122-5)
13. Hugall AF, O'Hara TD, Hunjan S, Nilsen R, Moussalli A. 2016 An exon-capture system for the entire class Ophiuroidea. *Mol. Biol. Evol.* **33**, 281–294. (doi:10.1093/molbev/msv216)
14. O'Hara TD, Stöhr S, Hugall AF, Thuy B, Martynov AV. 2018 Morphological diagnoses of higher taxa in Ophiuroidea (Echinodermata) in support of a new classification. *Eur. J. Taxon* **416**, 1–35. (doi:10.5852/ejt)
15. O'Hara TD, Thuy B, Hugall AF. 2021 Data from: Relict from the Jurassic: new family of brittle-stars from a New Caledonian seamount. Dryad Digital Repository. (doi:10.5061/dryad.18931zcx3)
16. Stamatakis A. 2014 RAxML Version 8: a tool for phylogenetic analysis and post-analysis of large phylogenies. *Bioinformatics* **30**, 1312–1313. (doi:10.1093/bioinformatics/btu033)
17. Bouckaert R, Heled J, Kühnert D, Vaughan T, Wu C-H, Xie D, Suchard MA, Rambaut A, Drummond AJ. 2014 BEAST 2: a software platform for Bayesian evolutionary analysis. *PLoS Comput. Biol.* **10**, e1003537. (doi:10.1371/journal.pcbi.1003537)
18. Mirarab S, Warnow T. 2015 ASTRAL-II: coalescent-based species tree estimation with many hundreds of taxa and thousands of genes. *Bioinformatics* **31**, i44–i52. (doi:10.1093/bioinformatics/btv234)
19. Kalyaanamoorthy S, Minh BQ, Wong TK, von Haeseler A, Jermiin LS. 2017 ModelFinder: fast model selection for accurate phylogenetic estimates. *Nat. Methods* **14**, 587–589. (doi:10.1038/nmeth.4285)
20. Sayyari E, Mirarab S. 2016 Fast coalescent-based computation of local branch support from quartet frequencies. *Mol. Biol. Evol.* **33**, 1654–1668. (doi:10.1093/molbev/msw079)
21. Degnan JH, Rosenberg NA. 2009 Gene tree discordance, phylogenetic inference and the multispecies coalescent. *Trends Ecol. Evol.* **24**, 332–340. (doi:10.1016/j.tree.2009.01.009)
22. Sanderson MJ. 2003 R8s: inferring absolute rates of molecular evolution and divergence times in the absence of a molecular clock. *Bioinformatics* **19**, 301–302. (doi:10.1093/bioinformatics/19.2.301)
23. Welch JJ, Bromham L. 2005 Molecular dating when rates vary. *Trends Ecol. Evol.* **20**, 320–327. (doi:10.1016/j.tree.2005.02.007)
24. Drummond AJ, Ho SYW, Phillips MJ, Rambaut A. 2006 Relaxed phylogenetics and dating with confidence. *PLoS Biol.* **4**, e88. (doi:10.1371/journal.pbio.0040088)
25. Rambaut A, Drummond AJ, Xie D, Baele G, Suchard MA. 2018 Posterior summarization in Bayesian phylogenetics using Tracer 1.7. *Syst. Biol.* **67**, 901–904. (doi:10.1093/sysbio/syy032)
26. Hoang DT, Chernomor O, von Haeseler A, Minh BQ, Vinh LS. 2018 UFBoot2: improving the ultrafast bootstrap approximation. *Mol. Biol. Evol.* **35**, 518–522. (doi:10.1093/molbev/msx281)
27. Felsenstein J. 2004 *Inferring phylogenies*. Sunderland, MA: Sinauer Associates.
28. Hendler G. 2018 Armed to the teeth: a new paradigm for the buccal skeleton of brittle stars (Echinodermata: Ophiuroidea). *Contrib. Sci.* **526**, 189–311.
29. Wilkie IC, Brogger MI. 2018 The peristomial plates of ophiuroids (Echinodermata: Ophiuroidea) highlight an incongruence between morphology and proposed phylogenies. *PLoS ONE* **13**, e0202046. (doi:10.1371/journal.pone.0202046)
30. Matsumoto H. 1917 A monograph of Japanese Ophiuroidea, arranged according to a new classification. *J. Coll. Sci. Imp. Univ. Tokyo* **38**, 1–408. pls 401–407.
31. Thuy B. 2013 Temporary expansion to shelf depths rather than an onshore-offshore trend: the shallow-water rise and demise of the modern deep-sea brittle-star family Ophiacanthidae (Echinodermata: Ophiuroidea). *Eur. J. Taxon* **48**, 1–242. (doi:10.5852/ejt.2013.48)
32. Okanishi M, Mah CL. 2020 Overlooked biodiversity from museum collections: four new species and one new genus of Ophiuroidea (Echinodermata) from Antarctica and adjacent regions with notes on multi-armed ophiuroids. *Mar. Biodiv.* **50**, 1–26. (doi:10.1007/s12526-020-01080-w)
33. Forest J, De Saint Laurent M, Chace FA. 1976 *Neoglyphea inopinata*: a crustacean "living fossil" from the Philippines. *Science* **192**, 884–884. (doi:10.1126/science.192.4242.884)
34. Forest J. 1981 Compte rendu et remarques générales. In *Résultats des campagnes MUSORSTOM: 1: Philippines (18–28 Mars 1976)*, pp. 9–50. Paris, ORSTOM.
35. Bribiesca-Contreras G, Verbruggen H, Hugall AF, O'Hara TD. 2017 The importance of offshore origination revealed through ophiuroid phylogenomics. *Proc. R. Soc. B* **284**, 20170160. (doi:10.1098/rspb.2017.0160)
36. Hess H, Thuy B. 2018 Emergence and early radiation of cyrtocrinids, with new species from a Lower to Middle Jurassic rock reef of Feuguerolles (Normandy, France). *Swiss J. Palaeontol.* **137**, 133–158. (doi:10.1007/s13358-018-0160-2)
37. Crisp MD, Cook LG. 2005 Do early branching lineages signify ancestral traits? *Trends Ecol. Evol.* **20**, 122–128. (doi:10.1016/j.tree.2004.11.010)
38. Clark MR *et al.* 2010 The ecology of seamounts: structure, function, and human impacts. *Ann. Rev. Mar. Sci.* **2**, 253–278. (doi:10.1146/annurev-marine-120308-081109)
39. O'Hara TD. 2007 Seamounts: centres of endemism or species-richness for ophiuroids? *Glob. Ecol. Biogeogr.* **16**, 720–732. (doi:10.1111/j.1466-8238.2007.00329.x)
40. O'Hara TD, Hugall AF, Woolley SNC, Bribiesca-Contreras G, Bax NJ. 2019 Contrasting processes drive ophiuroid phylodiversity across shallow and deep seafloors. *Nature* **565**, 636–639. (doi:10.1038/s41586-019-0886-z)
41. Pante E, France SC, Gey D, Cruaud C, Samadi S. 2015 An inter-ocean comparison of coral endemism on seamounts: the case of *Chrysogorgia*. *J. Biogeogr.* **42**, 1907–1918. (doi:10.1111/jbi.12564)
42. O'Hara TD, Thuy B, Hugall AF. 2021 Relict from the Jurassic: new family of brittle-stars from a New Caledonian seamount. FigShare.